STUDY OF A BATTERY-FREE PHOTOVOLTAIC HEAT PUMP WITH THERMAL ENERGY STORAGE

Yang Yufei, Ph.D. Candidate, Department of Human-Machine-Environment, Beijing University of Aeronautics and Astronautics, Beijing, China
Yuan Weixing, Associate Professor, Department of Human-Machine-Environment, Beijing University of Aeronautics and Astronautics, Beijing, China

Abstract: A battery-free photovoltaic heat pump powered by solar array directly is presented. The heat pump consists of solar array, DC/DC converter, brushless DC motor, vapor compression heat pump and water tank filled with phase change materials. To analyze the performance of the heat pump, a detailed model of the system is developed and numerically simulated. From the simulation results, the effects of ambient temperature, solar radiation and hot water temperature on the performance of the photovoltaic heat pump are shown and analyzed. The model could be used to predict the heating capacity, COP, compressor variable speed, and system efficiency for a real photovoltaic heat pump operated in various conditions.

Key Words: heat pump, photovoltaic, battery-free, compressor, phase change material

1 INTRODUCTION

The utilization of solar photovoltaic (PV) power to drive heat pump systems is considered to be one of the most promising areas of solar energy application. Despite its intermittency, solar energy is abundant, sustainable, and almost free of cost. With the price of solar cells reduced significantly in recent years, the cost of solar cells has been no more an obstacle to widespread commercialization of photovoltaic heat pumps. Photovoltaic heat pump is particularly suitable for domestic hot water supply and indoor air-conditioning in remote areas where electricity grid is unavailable.

Lead-acid batteries are now commonly used as energy storage devices in PV systems. But the lead-acid battery consists of lead, which is a toxic heavy metal, and acid, which is strongly corrosive. Both materials are harmful to environment. If lead-acid battery could be neglected, the solar powered heat pump will become much cheaper, and more friendly to environment. But when lead-acid battery is absent for such a system, it will brings some new problems. Firstly, as the output power of PV array varies constantly due to the intermittence of solar radiation and the fluctuation of temperature, the speed of the compressor should be adapted simultaneously in order to match the I-V characteristics of the PV array. That requires the compressor must be a variable speed one and some complicated electronic devices must be employed to regulate the compressor speed precisely. Secondly, as solar energy is intermittent, some other kind of energy storage method must be employed if the heat pump is required to use during night or in bad weathers. This can be solved by utilizing phase change materials (PCMs) in the water tanks. In the ordinary heat pumps, water can be heated during the day and stored in tanks, making hot water available at night or in cloudy days. Despite the simplicity of such a storage method, it is inefficient as its storage is in the form of sensible heat and the storage capacity is limited. In contrast, storing solar energy in suitable PCMs can offer high storage capacity (Al-Hinti et al. 2010).

In this article we study the performance of a battery-free photovoltaic heat pump with thermal energy storage. At first we give a brief description of the battery-free photovoltaic heat pump system. Then, we present a detailed mathematical model of the whole system. Finally, the model is solved and the simulation results are discussed. The parameters adopted in the simulation are all from the specifications of real commercial parts. The effects of ambient temperature, operating voltage and solar radiation on the compressor speed are discussed, and the effects of ambient temperature, hot water temperature (PCM melting temperature) and solar radiation on PV output power, heating capacity and COP are also analyzed.

2 DESCRIPTION AND MODELLING OF PHOTOVOLTAIC HEAT PUMP

The battery-free photovoltaic heat pump system with thermal energy storage analyzed in this paper is shown in Figure 1. The heat pump cycle consists of a variable speed DC compressor, a water-cooled condenser (which is a refrigerant-water heat exchanger), an electronic expansion valve, and an evaporator (which is a refrigerant-air heat exchanger). The compressor is driven by a brushless DC (BLDC) motor. To drive the BLDC motor, a special circuit board called BLDC driver is used.

The heat pump is directly powered by PV array and there is no storage battery in the system. To adapt the output voltage of PV array to the suitable voltage range of the compressor, a DC/DC converter is used between the PV array and the BLDC driver.

The heat pump produces hot water in the condenser during the day when there is sufficient solar radiation and stores heat in the water tank. The water tank is a well insulated cylindrical container filled with spherical capsules containing PCM modules. In the heat charging process, the hot water flows over the packed capsules from top to bottom and the PCM in the spherical capsules liquefies. In the discharging process, the PCM in the capsules solidifies and heats the water, which flows from bottom to top in the water tank.

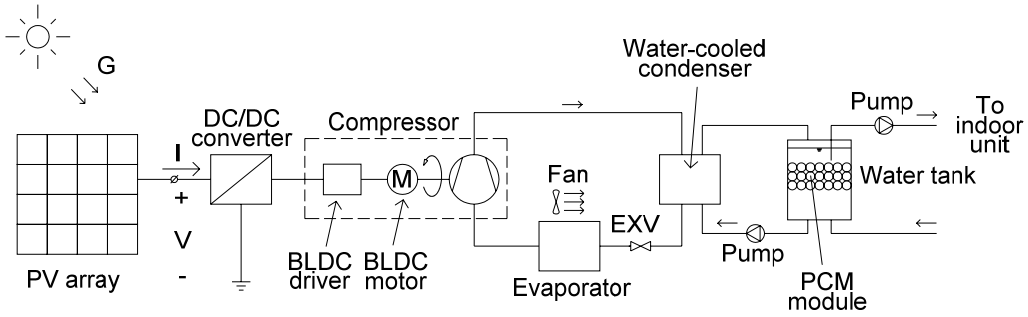


Figure 1: Schematic Diagram of the Battery-free Photovoltaic Heat Pump

2.1 PV Array

A PV array, also called a solar array, is a linked collection of solar cells in series and parallel. The cells convert solar energy into direct current electricity via the photovoltaic effect. The general model of a solar cell is described in Figure 2(a). The model consists of a photovoltaic current, a diode, a shunt resistor which represents leakage current, and a series resistor which represents cell internal resistance. Usually a simplified model of a solar cell is preferable, since the shunt resistance is very large and weighs little in analyzing the characteristics of solar cells. The simplified model of a solar cell is shown in Figure 2(b).

A single solar cell can yield only a limited voltage, usually 0.35~0.6V. So a series of solar cells must be linked in order to get a desired voltage. A series of solar cells linked in string called a PV module, which is shown in Figure 2(c).

The power that one module can produce is seldom enough to meet requirements of a heat pump, so the modules are linked in parallel to form an array. A PV array that has N_p parallel modules, each consisting of N_s solar cells in series is shown in Figure 2(d).

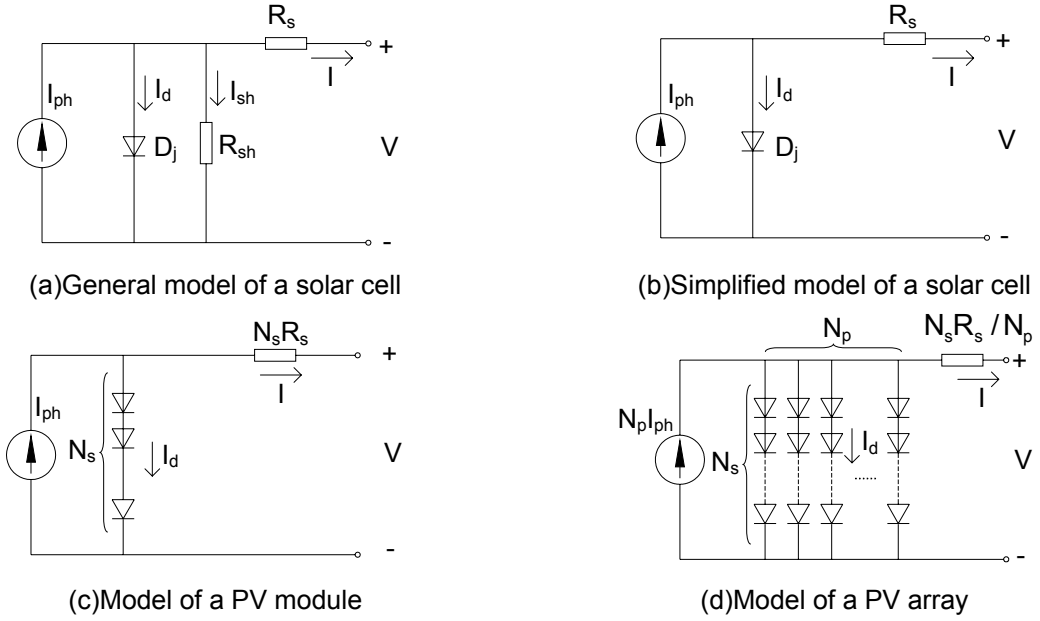


Figure 2: Equivalent Model of Solar Cell, Module and Array

The current output by a PV array is given by applying Kirchhoff's law, neglecting the shunt resistor, is

$$I = N_p \times I_{ph} - N_p \times I_d \tag{1}$$

The photovoltaic current I_{ph} is influenced by solar radiation and cell temperature. It can be determined by deploying reference temperature and reference radiation as written in equation (2) (Chenni et al. 2007)

$$I_{ph} = (G / G_{ref}) \times (I_{ph,ref} + \mu_{ISC} \times (T_c - T_{c,ref})) \tag{2}$$

where G(W/m^2) is solar radiation, T_c(K) is cell temperature. $I_{ph,ref}$ (A), G_{ref}(W/m^2), $T_{c,ref}$(K) are photovoltaic current, solar radiation and cell temperature at reference condition, respectively. μ_{ISC} (A/K) is temperature coefficient of short circuit current. I_d(A) is diode current, which is determined by Shockley equation:

$$I_d = I_0 \times (\exp(q \times (V + I \times N_s \times R_s / N_p) / (k \times N_s \times A \times T_c)) - 1) \tag{3}$$

where I_0 is reverse saturation current of diode; q(= 1.602×10^{-19} Coulomb) is electron charge; A is completion factor(for monocrystalline silicon is 1.2 and for polycrystalline silicon is 1.35); k(= 1.381×10^{-23} J/K) is Boltzmann's constant. The reverse saturation current is related to cell temperature. It can be determined by comparing with reference condition, that is

$$I_0 = I_{0,ref} \times (T_c / T_{c,ref})^3 \times \exp(q \times E_g / k / A \times (1/T_{c,ref} - 1/T_c)) \tag{4}$$

where $I_{0,ref}$ (A) is saturation current at reference condition; E_g is cell material bandgap energy, for silicon it is 1.12eV. Given array open-circuit voltage at reference temperature $V_{oc,ref}$, the reverse saturation current at reference temperature can be written as below(Tsai et al. 2008).

$$I_{0,ref} = I_{sc,ref} \times \exp(-q \times V_{oc,ref} / k / A / T_{c,ref}) \quad (5)$$

Since $I_{ph} >> I_0$, by ignoring the diode the photovoltaic current is approximately equal to the short-circuit current, i.e.,

$$I_{ph,ref} = I_{sc,ref} \quad (6)$$

The series resistance N_s is an important parameter in PV array simulation, which can be calculated by equation (7), where $V_{m,ref}$, $I_{m,ref}$ are voltage and current at maximum power point at reference condition, respectively.

$$N_s \times A = q \times (V_{m,ref} + I_{m,ref} \times N_s / N_p \times R_s - V_{oc,ref}) / (k \times T_{c,ref} \times \ln(1 - I_{m,ref} / I_{sc,ref})) \quad (7)$$

To predict the energy efficiency of photovoltaic heat pump, it is useful to relate cell temperature to ambient temperature. Approximately, they have the following relationship (Zhengming et al. 2005):

$$T_c = T_a + 0.03 \times G \quad (8)$$

where T_a is ambient temperature. The output power of PV array is defined as

$$P = V \times I \quad (9)$$

PV array efficiency is defined as

$$\eta_{PV} = P / (G \times A_t) \quad (10)$$

where A_t is the total area of PV array that receives solar radiation.

2.2 DC/DC Converter

PV array is a nonlinear power source; it has a single maximum power point (MPP) under certain solar radiation and temperature. The working point of PV array may deviate from the MPP when solar radiation or temperature changes. That causes efficiency loss of PV array. In order to improve the overall efficiency of PV system, one important way is real-time adjustment of the working point, making the PV array always work in the vicinity of the maximum power point. This process of seeking the maximum power point is called maximum power point tracking (MPPT).

There are several algorithms to realize maximum power point tracking (Salas et al. 2006), but for photovoltaic heat pump the conventional and simple method of constant voltage tracking (CVT) is practicable. First, the working voltage of compressor must be stable, as over-voltage and under-voltage are both hazardous to the compressor and the heat pump. Second, within a certain range, the operating voltage corresponding with the maximum power point changes little when solar radiation changes. According to this feature, it is possible to make a certain impedance transformation between the PV array and the load, making the system to be a voltage regulator. By maintaining the operating voltage of PV array at the voltage corresponding with the MPP, the output power is kept close to the maximum power. This method is not precise, since the maximum power point is not only

affected by solar radiation but also affected by temperature, but it is enough to be used in photovoltaic heat pump applications.

The CVT is realized by the DC/DC converter that presents an optimal electrical load to the PV array and produces a voltage suitable for the compressor. The output voltage of DC/DC converter is defined as

$$V_d = \alpha \times V \tag{11}$$

where α is duty cycle of DC/DC converter ($0 < \alpha < 1$). By applying energy balance, the output power of DC/DC converter is defined as

$$P_1 = \eta_{DC} \times P \tag{12}$$

where η_{DC} is conversion efficiency of DC/DC converter.

2.3 BLDC Driver and BLDC Motor

The compressor motor considered here is a permanent magnet brushless DC motor. BLDC motors do not use brushes for commutation; instead, they are electronically commutated. BLDC motors have many advantages over brushed DC motors and induction motors for they have better speed-torque characteristics, higher dynamic response and efficiency, longer operating life, quieter operation and higher speed ranges. In addition, the ratio of torque delivered to the size of the motor is higher, making it suitable for using in photovoltaic heat pump applications. The electric power input a BLDC motor is calculated by

$$P_1 = V_d \times I_a \tag{13}$$

where V_d (V) is output voltage of DC/DC converter and the bus voltage of BLDC driver, I_a (A) is wire current of BLDC motor. P_1 consists of three components:

$$P_1 = K_T \times I_a \times \omega + r_a \times I_a^2 + \Delta U \times I_a \tag{14}$$

where K_T is torque constant(Nm/A); ω, motor mechanical speed(rad/s); r_a, winding resistance(Ω); ΔU, voltage drop caused by electronic commutation circuit in the BLDC driver(V). The first term of the right side of Eq.(14) represents the electromagnetic power P_e, while the second and third term account for power loss due to winding resistance (copper loss), and power loss due to electronic commutation circuit, respectively.

The electromagnetic power P_e can be written as

$$P_e = (T_L + T_0) \times \omega = P_2 + P_0 \tag{15}$$

where T_L is load torque; T_0 is no-load torque, $T_0=P_0/\omega$; P_2 is useful power output to compressor; P_0 is no-load loss, including iron core loss and mechanical friction loss. The BLDC motor efficiency is defined as (Changliang 2009)

$$\eta_{motor} = P_2 / P_1 = 1 - r_a / U_d \times I - (P_T + P_0) / U_d / I \tag{16}$$

2.4 Heat Pump Cycle

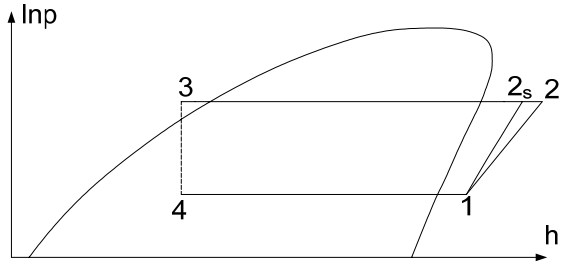


Figure 3: Pressure-enthalpy Diagram for R-134a

The heat pump cycle employing refrigerant R-134a is shown in Figure 3. To evaluate the cycle, we should firstly determine the evaporating temperature T_{evap} and condensing temperature T_{cond}, which are primarily determined by the ambient temperature and hot water temperature:

$$T_{evap} = T_a - \Delta T_e \ , \quad T_{cond} = T_w + \Delta T_c \tag{17}$$

where T_w is hot water temperature at condenser outlet. ΔT_e and ΔT_c are heat transfer temperature difference in evaporator and condenser, respectively. After decision of evaporating temperature and condensing temperature, the evaporating pressure and condensing pressure corresponding to the evaporating and condensing temperature can then be determined. The temperature at compressor inlet T_1 and condenser outlet T_3 can be determined by giving superheating degree ΔT_{sup} and subcooling degree ΔT_{sub}:

$$T_1 = T_{evap} + \Delta T_{sup} \ , \ T_3 = T_{cond} - \Delta T_{sub} \tag{18}$$

The enthalpy at compressor inlet is

$$h_1 = h(T = T_1, P = P_{evap}) \tag{19}$$

Identifies state 2s as isentropic and we get

$$h_{2s} = h(P = P_{cond}, S = S_1) \tag{20}$$

where S_1 is specific entropy of refrigerant at point 1. By applying energy balance on isentropic compression process, we get

$$h_1 + w_{cs} = h_{2s} \tag{21}$$

where w_{cs} is theoretical specific power consumption of compressor(J/kg/K). By giving isentropic efficiency η_c , the actual specific power consumption of compressor is

$$w_c = w_{cs} / \eta_c \tag{22}$$

Apply energy balance on real compression process, assumed adiabatic

$$h_1 + w_c = h_2 \tag{23}$$

The actual work input the compressor $\dot{W}_c$ is calculated by

$$W_c = \dot{m} \times w_c \tag{24}$$

The mass flow rate of refrigerant $\dot{m}$ is calculated at the compressor suction port (kg/s):

$$\dot{m} = n/60 \times V_c \times \eta_\upsilon / \upsilon_1 \times 10^{-6} \tag{25}$$

where n is compressor speed(rpm), $n = 30 \times \omega / \pi$; V_c is displacement of compressor(cm^3); η_υ is volumetric efficiency of compressor; υ_1 is specific volume of refrigerant gas at compressor suction port (m^3/kg).

The heating capacity of heat pump is calculated by

$$Q_h = \dot{m} \times (h_2 - h_3) \tag{26}$$

The coefficient of performance of the heat pump is defined as

$$COP_h = Q_h / W_c \tag{27}$$

2.5 Water Tank with PCM Module

The melting point of PCM is determined by the available maximum condensing temperature of the heat pump, it must be several degrees lower than the condensing temperature. The average thermal power charged into the tank with PCM modules is defined as (Medrano et al. 2009):

$$Q_{PCM} = M \times (cp_s \times (T_{low} - T_{ini}) + H_{PCM} + cp_l \times (T_{end} - T_{up})) / \tau \tag{28}$$

where M(kg) is the mass of PCM, cp_s (J/kg·K) and cp_l (J/kg·K) are specific heat capacities of PCM at solid and liquid state, respectively. T_{low} and T_{up} are the lower and upper temperature values of the PCM phase change range, T_{ini} and T_{end} are the PCM temperatures at the initial and end of the phase change process, respectively. H_{PCM} (J/kg) is the phase change enthalpy of PCM. τ is the time of a charging process until complete melting.

2.6 System Efficiency

The overall efficiency of the photovoltaic heat pump is the product of h_{PV}, h_{DC}, h_m and COP_{hp}:

$$h_{SYS} = h_{pv} \eta h_{DC} \eta h_{motor} \eta COP_{hp} \tag{29}$$

It can be seen that the system overall efficiency is determined by solar array efficiency, DC/ DC conversion efficiency, DC motor efficiency and heat pump COP.

3 SIMULATION RESULTS AND DISCUSSIONS

In the simulation, the set of system components models including PV array, DC/DC converter, BLDC motor, and heat pump is solved by numerical method. Thermophysical properties of refrigerant R-134a are used to determine the status of each point of the refrigeration cycle, making the simulation results close to real results.

The parameters of compressor employs the specifications of Aspen 14-24-000X, which is a miniature, variable speed rotary compressor. The nominal voltage of the compressor is 24V

DC and the voltage range is 20~30V DC. The compressor employs a 10-pole BLDC motor which can operate at a wide speed range from 2000 to 6500rpm. The compressor speed can be easily controlled just by supplying the BLDC driver board an analog voltage signal that ranges from 0 to 5V. All these features make it very suitable for photovoltaic heat pump applications. The displacement of the compressor is 1.4 cm^3. The compressor volumetric efficiency is considered to be 0.85 and the isentropic efficiency is considered to be 0.92. The BLDC motor parameters used in the simulation are: K_T=0.026Nm/A, L_a=0.14mH, r_a=0.24Ω, ΔU=0.7V, T_L=0.14Nm.

The heat transfer temperature difference of air heat source evaporator is configured to be 15K and temperature difference of water-cooled condenser is configured to be 5K, which are close to the conditions of real heat pumps. The superheating degree at compressor inlet is designated as 6K and the subcooling degree at condenser outlet is designed as 3K in the simulation.

The efficiency of DC/DC converter adopted here is 87%, which is close to the value of a real DC/DC converter. The simulation parameters of the PV array are listed in Table 1.

Table 1: Simulation Parameters at Reference Conditions

Parameter	Value	Parameter	Value	Parameter	Value
A	1.3	$I_{sc,ref}$	5.55A	$V_{m,ref}$	26.5V
A_t	0.875m^2	N_p	1	$V_{oc,ref}$	33.2V
G_{ref}	1000 W/m^2	N_s	57	μ_{ISC}	0.003 A/K
$I_{m,ref}$	4.95A	$T_{c,ref}$	321K	μ_{VOC}	-0.73V/K

The properties of PV array are apparently nonlinear as shown in Figure 4 and Figure 5. Figure 4 shows the output current and power of PV array depend on the operating voltage and solar radiation. At a specified voltage, the stronger the solar radiation is, the higher the output current and power are. The output power reaches the highest almost at the same voltage of around 27V, which is the optimal working voltage corresponding with the maximum power points. Figure 5 shows the effect of ambient temperature on the output current and power of PV array. It is clear that as ambient temperature decreases the output current and power increase with higher voltages more than 25V. This is not true when the voltage is low, but the variation is very limited.

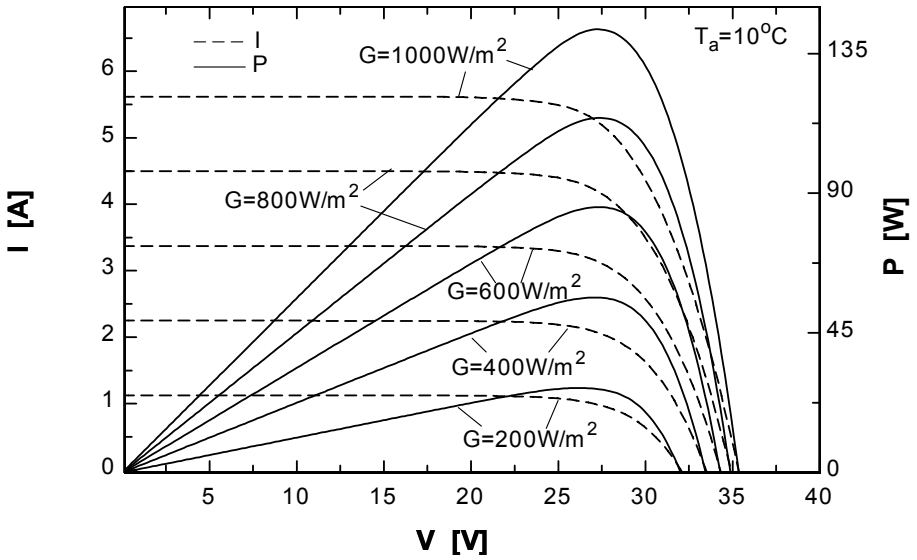


Figure 4: Effect of Solar Radiation on PV Array Characteristics

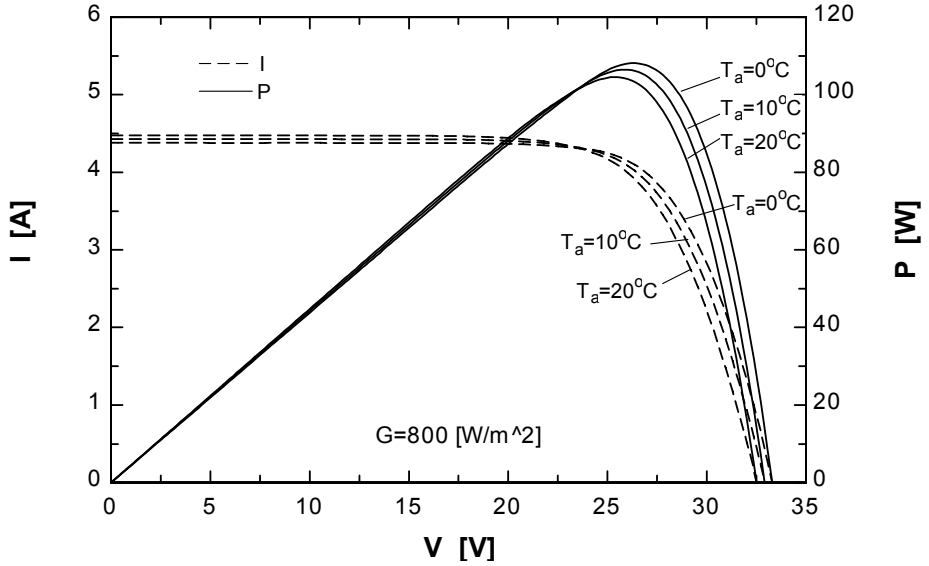


Figure 5: Effect of Ambient Temperature on PV Array Characteristics

Figure 6 shows the variations of motor speed and motor efficiency with respect to output voltage of PV array under different solar radiations. Under a specified solar radiation, the BLDC motor reaches a maximum rotation speed in a certain voltage around 27V, which is consistent with the optimal working voltage of PV array. But the efficiency of BLDC motor always increases with the increment of voltage.

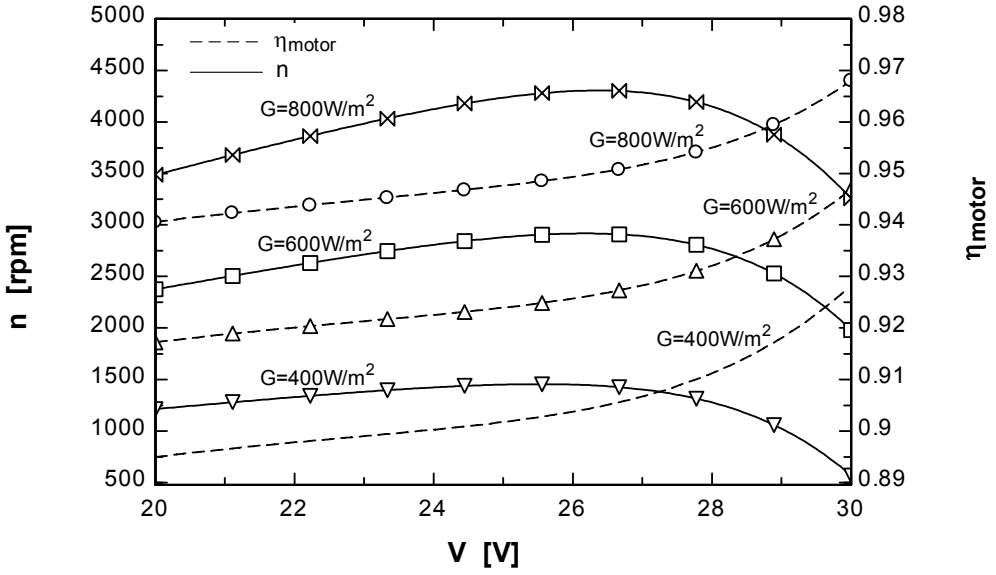


Figure 6. Effects of Voltage and Solar Radiation on Motor Speed and Motor Efficiency

Figure 7 shows the effect of ambient temperature on the speed and efficiency of BLDC motor, with PV array output voltage as independent variable. Under higher working voltages, the speed of BLDC motor increases with the decrement of ambient temperature, which is consistent with the P-V characteristic of PV array. On the contrary, the efficiency of BLDC motor increases as the ambient temperature increases, under higher voltages.

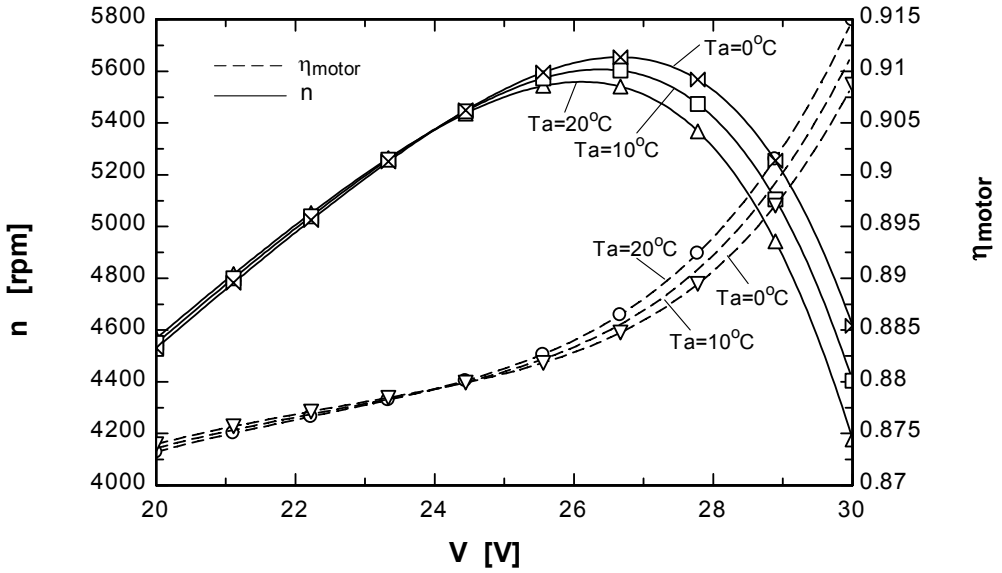


Figure 7. Effects of Voltage and Ambient Temperature on Motor Speed and Efficiency

Figure 8 shows the variations of heating capacity and the coefficient of performance of the heat pump COP_h with respect to output voltage of PV array under different ambient temperatures. From the figure, we know that the heating capacity is influenced by both output voltage and ambient temperature. Both heating capacity and coefficient of performance increase as ambient temperature rises. And under a given ambient temperature, the heating capacity reaches maximum at a certain output voltage. The coefficient of performance of heat pump is almost not affected by output voltage of PV array. That is because the COP_h is mainly determined by ambient temperature and hot water temperature. When heating capacity decreases, the power consumption also decreases in the same ratio.

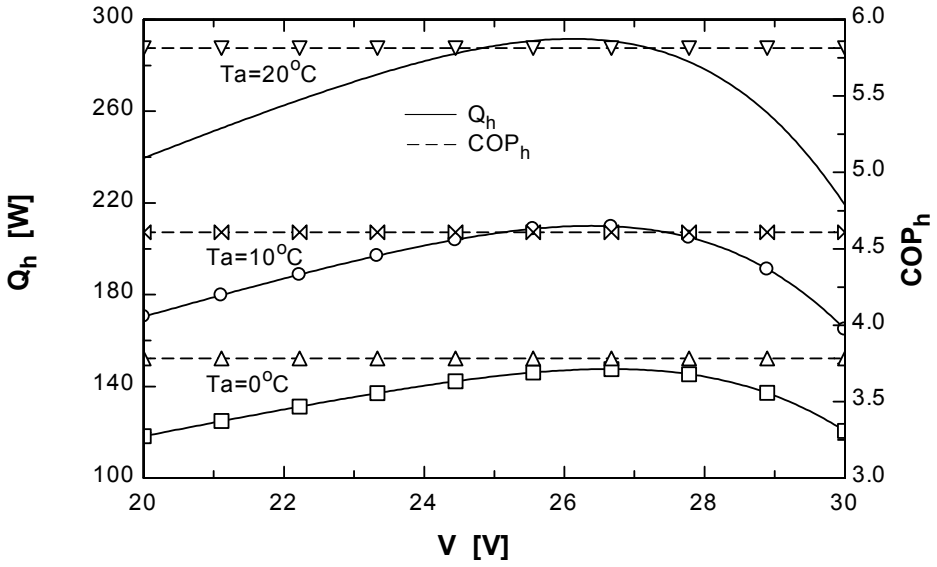


Figure 8. Effects of Voltage and Ambient Temperature on Heating Capacity and COP

Figure 9 shows the variation of heat pump COP with respect to ambient temperature under different hot water temperatures. Heat pump COP increases as ambient temperature rises. And the higher the hot water temperature is, the lower the heat pump COP.

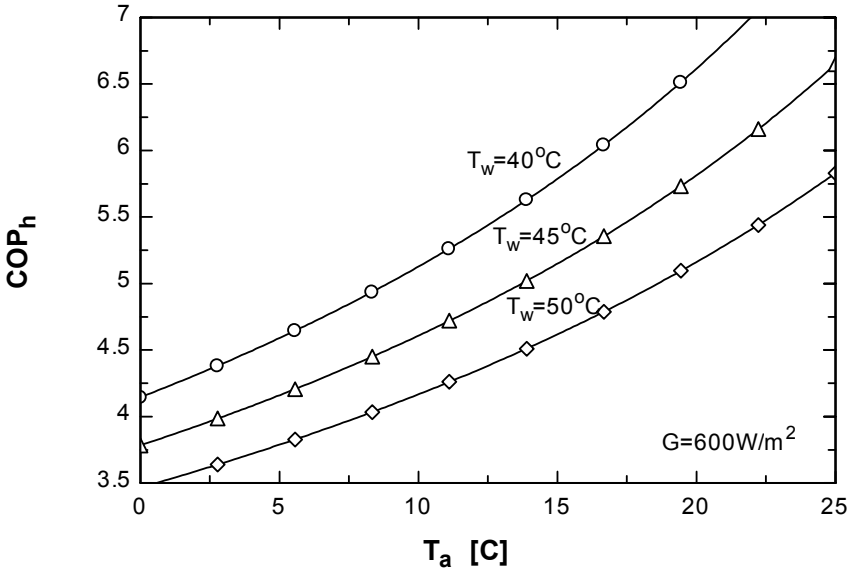


Figure 9. COP_h vs. Ambient Temperature

Figure 10 shows the variation of the system overall efficiency η_{sys} with respect to ambient temperature under different hot water temperatures. Similar to heat pump COP, the system efficiency also increases as ambient temperature rises and decreases as hot water temperature increases. It shows that the system overall efficiency is mainly determined by the efficiency of the heat pump cycle. Although the PV array has higher photovoltaic efficiency at lower ambient temperature, the efficiency of heat pump drops greatly at lower ambient temperature and thus diminishes the efficiency rise in the PV array.

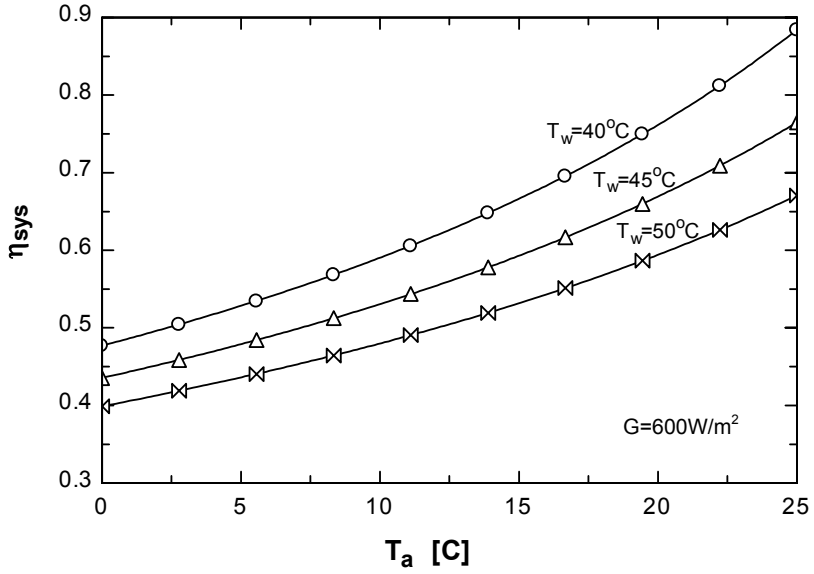


Figure 10. System Efficiency vs. Ambient Temperature

4 CONCLUSIONS

A detailed model of a battery-free photovoltaic heat pump system including PV array, DC/DC converter, BLDC motor, vapor compression heat pump and water tank with PCM modules has been developed. The proposed model takes solar radiation, ambient temperature and hot water temperature as input parameters. The simulation results output the I-V, P-V and n-

V characteristics of the photovoltaic heat pump. The model could be used to predict the variation of heating capacity, compressor speed, heat pump COP, and system efficiency for a real photovoltaic heat pump operated in various conditions. The phase change process of the PCMs in the water tank is not included in the simulation this time, which will be added in the future studies.

5 REFERENCES

Huan-Liang Tsai, Ci-Siang Tu, and Yi-Jie Su. 2008. “Development of generalized photovoltaic model using MATLAB/SIMULINK,” Proceedings of the World Congress on Engineering and Computer Science

I. Al-Hinti, A. Al-Ghandoor, A. Maaly and I. Abu Naqeera. 2010. “Experimental investigation on the use of water-phase change material storage in conventional solar water heating systems,” Energy Conversion and Management, Vol. 51, pp1735-1740.

M. Medrano, M.O. Yilmaz, M. Nogues, I. Martorell, Joan Roca and Luisa F. Cabeza. 2010. “Experimental evaluation of commercial heat exchangers for use as PCM thermal storage systems,” Applied Energy, Vol.86, pp2047-2055

R. Chenni, M. Makhlouf, T. Kerbache and A. Bouzid. 2007. “A detailed modelling method for photovoltaic cells,” Energy, Vol. 32, pp1724-1730

V.Salas, E.Olias, A. Barrado, A. Lazaro. 2006. “Review of the maximum power point tracking algorithms for stand-alone photovoltaic systems,” Solar Energy Materials & Solar Cells, Vol.90, pp1555-1578

Xia Changliang, 2009. Control Systems of Brushless DC Motors, Science Press, Beijing

Zhao Zhengming, Liu Jianzheng, Sun Xiaoying and Yuan Liqiang. 2005. Solar Photovoltaic Power Generation and Applications, Science Press, Beijing